Non-stoichiometric AlO$_x$ Films Prepared by Chemical Vapor Deposition Using Dimethylaluminum Isopropoxide as Single Precursor and Their Non-volatile Memory Characteristics

**Sun Sook Lee,[†] Eun-Seok Lee,[†] Seok Hwan Kim,[†] Byung Kook Lee,[†,‡] Seok Jong Jeong,[†]
Jin Ha Hwang,[‡] Chang Gyoun Kim,[†] Taek-Mo Chung,[†] and Ki-Seok An[†,*]**

[†] *Advanced Materials Devision, Korea Research Institute of Chemical Technology, P.O. Box 107, Yuseong,
Daejeon 305-600, Korea. *E-mail: ksan@krict.re.kr*
[‡]*Department of Materials Science and Engineering, Hongik University, Seoul 121-791, Korea*

Dimethylaluminum isopropoxide (DMAI, (CH$_3$)$_2$AlO^{i}Pr) as a single precursor, which contains one aluminum and one oxygen atom, has been adopted to deposit non-stoichiometric aluminum oxide (AlO$_x$) films by low pressure metal organic chemical vapor deposition without an additional oxygen source. The atomic concentration of Al and O in the deposited AlO$_x$ film was measured to be Al:O = ~1:1.1 and any serious interfacial oxide layer between the film and Si substrate was not observed. Gaseous by-products monitored by quadruple mass spectrometry show that β-hydrogen elimination mechanism is mainly contributed to the AlO$_x$ CVD process of DMAI precursor. The current-voltage characteristics of the AlO$_x$ film in Au/AlO$_x$/Ir metal-insulator-metal (MIM) capacitor structure show high ON/OFF ratio larger than ~10^6 with SET and RESET voltages of 2.7 and 0.8 V, respectively. Impedance spectra indicate that the switching and memory phenomena are based on the bulk-based origins, presumably the formation and rupture of filaments.

Key Words : Non-stoichiometric AlO$_x$, Dimethylaluminum isopropoxide (DMAI), Single precursor, β-Hydrogen elimination, Non-volatile memory

Introduction

Chemical vapor deposition (CVD) has been regarded as one of promising techniques for high quality thin films because it has some advantages over other methods such as good uniformity, controllability of thickness with a low defect density, and better step coverage, *etc.*[1] Normally, stoichiometric films can be prepared by suitable thermal decomposition and chemical reaction of well-designed metal precursors and reactants on substrates.

On the other hand, a simple way for the deposition of proper films at suitable temperature in CVD process has been pursued using well-designed single precursor without an extra reactant.[2-4] Generally, for the CVD process with single precursor, well-designed and -synthesized precursors including both metal and reactant elements with suitable chemical bonds were essentially required. An ideal single precursor should leave only proper elements to form thin films by spontaneous thermal decomposition reaction on the substrate without the recombination of by-products because of the absence of extra reactants. Comparing with normal CVD process, the CVD process with single precursor may have several merits, such as well-defined interface between the deposited film and the substrate, relatively low deposition temperature, and easy formation of stoichiometric and sub-stoichiometric films caused only by the design of precursor.

Several CVD processes and thermal decomposition reaction mechanisms of oxides and nitrides with single pre-

cursors have been well established.[4-6] In particular, β-hydrogen elimination mechanism has been studied as a typical decomposition and chemical reaction process in the CVD processes of oxides with alkyl metal alkoxides (RMOR) as a single precursor.[4,5,7]

Recently, semiconductor devices often require artificial sub-stoichiometric films in order to create or enhance unique physical and chemical properties of the films.[8-10] In the case of conventional CVD processes, controlling the amount of an extra reactant may be the only method to deposit sub-stoichiometric films, in which it is very difficult to control exactly the sub-stoichiometric compositional ratio between the elements within the films. Although main researches for the CVD process with single precursor have been focused on preparing the stoichiometric oxides and nitrides, it can be also useful to develop the CVD process for the sub-stoichiometric films through the suitable choice or synthesis of single precursor.

One of precursors for aluminum oxide films is dimethylaluminm isopropoxide (DMAI, (CH$_3$)$_2$AlO^{i}Pr), which consists of one aluminum, one oxygen atom and carbon species and has good chemical properties such as high vapor pressure and non-pyrophoric, *etc.* DMAI precursor was employed to grow Al$_2$O$_3$ films by CVD as single precursor[5] and by atomic layer deposition (ALD) with H$_2$O.[11]

As one of the promising candidates of next-generation non-volatile memory (NVM), resistive random access memory (ReRAM) has a great potential because of simple device

structure, low power consumption, high density integration, high-speed writing/erasing, and long retention time, *etc.* Resistance switching phenomenon has been observed on various kinds of binary oxides and perovskite oxides, such as NiO,[12,13] TiO_2,[14] Nb_2O_5,[15] Al_2O_3,[16,17] CuO_x,[8] ZrO_x,[9] MgO_x,[10] Cr-doped $SrTiO_3$, and $SrZrO_3$, *etc.*[18,19] Although detail mechanism of the resistance switching phenomenon has not yet been clearly elucidated, it is expected that the resistive switching properties are related to defects in several non-stoichiometric oxide films.[8-10,12-15]

In this study, as one of efforts for syntheses and applications of chemically well-designed metal-organic compounds to fabricate thin film materials, we report the deposition of non-stoichiometric aluminum oxide (AlO_x) films by low pressure CVD using DMAI as single precursor and possible applicability of non-volatile ReRAM device. The non-volatile resistive switching properties of $Au/AlO_x/Ir$ metal-insulator-metal (MIM) capacitor structure were tested by current-voltage (I-V) measurement and ac impedance spectroscopy. Finally, we discuss the thermal decomposition and reaction mechanism of DMAI precursor during the AlO_x CVD process by analysis of gaseous by-products using quadruple mass spectrometry (QMS).

Experimental Details

In order to exclude additional oxidation caused by residual oxygen source during the deposition of aluminum oxide films, a high vacuum chamber was used. The base pressure before the deposition was kept lower than $\sim 2 \times 10^{-6}$ torr and the working pressure was maintained at $\sim 3 \times 10^{-4}$ torr during the deposition. DMAI precursor and gas flow line were retained at 60 °C, respectively. Any carrier gas was not used to deliver DMAI precursor because of enough vapor pressure (25 °C, 0.85 torr) of DMAI precursor (for the deposition). The substrate temperature was varied in the range of 300-550 °C. Each deposition was carried out for 30 min.

Depth profiling Auger electron spectroscopy (AES) and X-ray photoelectron spectroscopy (XPS) were employed to investigate the atomic concentration of aluminum and oxygen and chemical environment as well as carbon contamination of the deposited films. High resolution transmission electron microscopy (TEM) was employed to investigate the interfacial reaction between the deposited aluminum oxide and Si substrate.

The thermal decomposition mechanism of DMAI precursor on the substrate was investigated by QMS. In order to ensure enough thermal reaction pathway and gaseous by-products during the delivery of DMAI precursor, small pieces of Si wafer were fully filled at long (45 cm) length and small diameter (< 5 mm) quartz tube covered with a temperature controllable furnace. Both sides of the quartz were connected to the bottle of the precursor and the high vacuum chamber equipped with QMS, respectively, with the precession leakage control valves. Before the QMS measurement, enough bake-out was carried out at 150 °C in

order to remove the residual water in the system and the precursor was also purged by freeze-pump-thaw cycle. During the measurement, the precursor was heated at 60 °C.

In order to measure the resistive switching properties, AlO_x films were deposited on $Ir/TiN/SiO_2/Si$ substrates at 450 °C. After AlO_x film deposition, Au top electrodes with a diameter of approximately 200 μm using metal shadow masks were deposited in order to fabricate the MIM capacitor. Resistive switching was measured using a Keithley source/ measure unit, KE286 with controllable compliance in current, *e.g.* maximum 100 mA.

The ac characteristics were monitored using impedance spectroscopy to resolve the origin of switching behaviors in AlO_x thin films. Impedance spectra were acquired using a low-frequency impedance analyzer (HP4192A, Palo Alto, CA). The frequency sweeping was performed between 1 MHz and 100 Hz in the logarithmic manner, ten points per decade. DC current-voltage measurements were made using a source-meter unit (Keithley 236, Cleveland, OH) in combination with the controlled compliance in the "current" mode.

Results and Discussion

Figure 1 shows the result of depth profiling AES for the aluminum oxide films (~ 450 Å) deposited on the Si(100) substrate at 450 °C. As shown in Fig. 1, the atomic ratio of Al:O was estimated to be ~1:1.1 and the ratio was not considerably changed within the films. It is worthwhile to note that the carbon contamination is negligible inside the films. Generally, the carbon contamination in the CVD process is enhanced by improper thermal decomposition of the precursor and/or undesirable recombination of by-products. The atomic concentration of Al:O and the negligible carbon incorporation suggest that the thermal decomposition of DMAI precursor at 450 °C is quite suitable to the CVD process of non-stoichiometric AlO_x films. In previous FT-IR[20] and temperature-programmed desorption (TPD) studies[21] for the thermal reaction and decomposition of DMAI pre-
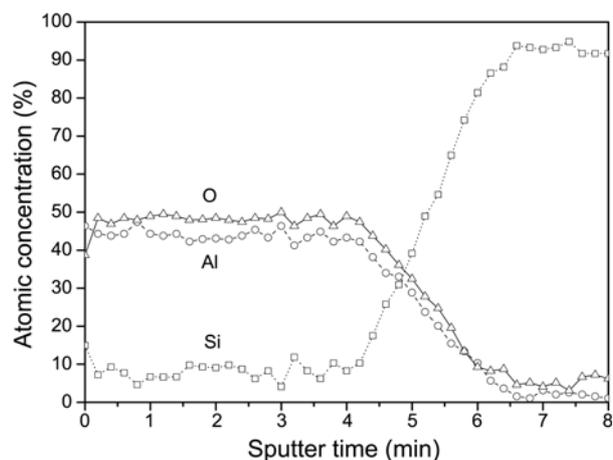
Figure 1. AES depth profile of AlO_x films deposited on the Si(001) substrate at 450 °C.
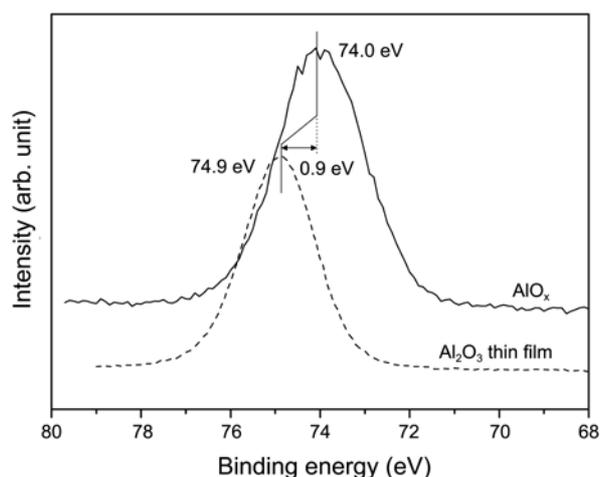
Figure 2. Al 2p core level spectra for AlO$_x$ films deposited at 450 °C and Al$_2$O$_3$ film deposited by DMAI-H$_2$O ALD. The XPS spectra were obtained after Ar$^+$ sputtering of 5 min.

Figure 3. TEM image of AlO$_x$ film grown on Si substrate at 450 °C.

cursor also described that the reaction temperature was higher than 400 °C.

In Figure 2, Al 2p core level spectrum of the AlO$_x$ films deposited at 450 °C was compared with that of Al$_2$O$_3$ film deposited by DMAI-H$_2$O ALD process.[11] The binding energy (BE) positions of Al 2p peaks of AlO$_x$ and Al$_2$O$_3$ film were measured to be 74.0 and 74.9 eV, respectively. By the difference of electronegativity of Al and O, the BE of Al 2p core level shifts to higher at higher oxidation state. As expected in AES result of Figure 1, the lower BE position of AlO$_x$ films implies that the oxidation state of the AlO$_x$ films is lower than that of Al$_2$O$_3$. Our XPS results are well consistent with the previous XPS related to the oxidation states of Al metal.[22,23]

DMAI precursor consists of one aluminum with two methyl (CH$_3$) and one isopropoxy and exists as a dimer in the liquid phase at room temperature.[24] In the previous FT-IR measurement for thermal decomposition of DMAI precursor, it was found that DMAI precursor starts to be decomposed at ~500 °C and, in particular, the Al-O bond is mainly decomposed above 540 °C.[20] This implies that the DMAI precursor can be well applied as the single precursor for aluminum oxide film at lower reaction temperature than 540 °C.

In the previous CVD process using DMAI single precursor, Koh *et al*.[6] reported the formation of Al$_2$O$_3$ films on the Si substrates at high base pressure of 1 Pa. Different to our result shown in Figure 1, the atomic ratio by depth-profiling AES for the deposited films at 400 °C measured to be Al:O = 2:3, although exact oxidation state of Al by XPS was not compared. Considering the thermal decomposition behavior of DMAI precursor, which presumably follows the β-hydrogen elimination mechanism; it is not possible to form stoichiometric Al$_2$O$_3$ film by a simple thermal decomposition at low reaction temperature. As one possible explanation for the different Al/O atomic ratio concentration, it may be difficult to exclude an additional reaction
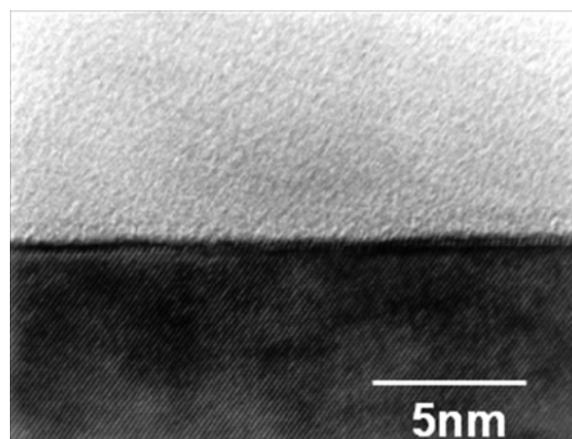
with residual oxygen species in the previous Al$_2$O$_3$ CVD process[6] due to much higher base pressure of 1 Pa than our deposition condition.

Figure 3 shows cross-sectional TEM image for AlO$_x$ thin films on the Si substrate deposited at 450 °C. In the TEM image, the interface between the deposited AlO$_x$ and Si substrate is sharply separated without the formation of other interfacial oxide layer. In normal CVD/ALD process for oxide films, depending on the substrate temperature, the exposure of Si substrate to the reactant gas of oxygen at high temperature often results in the inter-diffusion of oxygen and/or metal to the sub-surface layers of Si substrate and the formation of undesired Si oxide and/or silicate layers at the interface.[25]

On the other hand, as one of expected merits for the CVD process with single precursor, sharp interface can be formed almost without the oxidation of sub-surface of Si substrate if the single precursor is well operated at suitable temperature. Because oxygen atom bonds already to metal atom in the single precursor, the inter-diffusion of oxygen to Si substrate is much more difficult than the use of separate O$_2$ gas in the metal oxide CVD process.

To investigate the CVD reaction mechanism of the DMAI
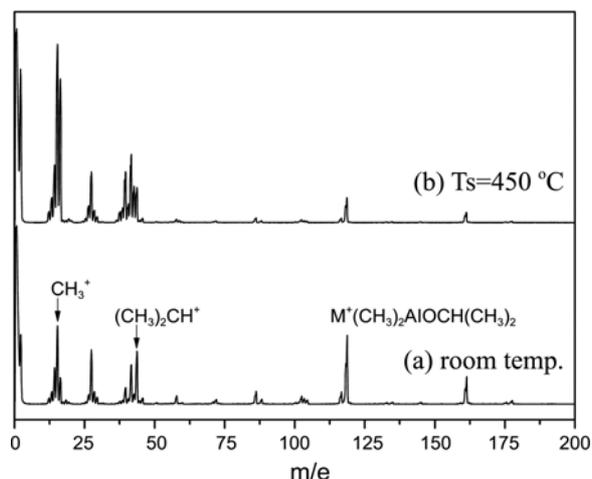
Figure 4. Mass spectra of DMAI (a) at room temperature and (b) after thermal reaction at 450 °C.
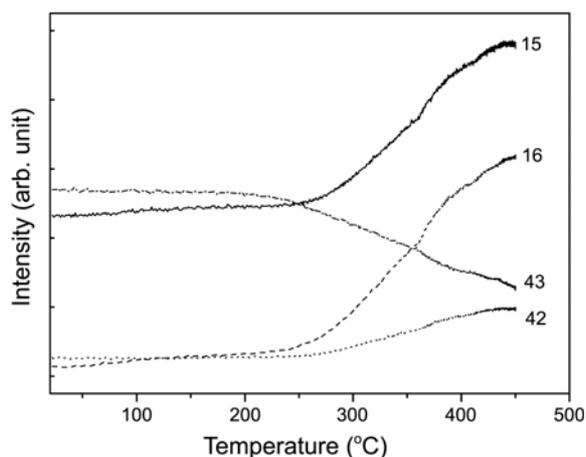
Figure 5. Temperature programmed desorption spectrum of various species obtained during the deposition process.

Scheme 1. Proposed decomposition mechanism of DMAI precursor following β-hydrogen elimination by CVD reaction.

single precursor in the AlO_x film growth, the reaction products during the deposition at 450 °C were analyzed by *in-situ* QMS. Figure 4 shows mass spectra (a) before and (b) after the CVD reaction during the exposure of DMAI precursor. In Figure 4(a), although the mass peak corresponding to DMAI dimer (m/e = 236 amu) itself were not detected because of the detection limit of our QMS (m/e < 200), the appearance of mass peak around 160 amu larger than that of DMAI monomer (118 amu) indicates that the precursor is exposed as a dimer-type. The mass peaks at m/e = 15, 16, 42, and 43 amu are originated from methyl (CH_3), methane (CH_4), propene ($CH_3CH=CH_2$), and isopropyl (($CH_3)_2CH$), respectively. At the reaction temperature of 450 °C, the relative peak intensities of methyl, methane, propene, and isopropyl, changed with considerable decrease of the peak intensity of DMAI monomer.

Based on the changes of the mass spectrum shown in Figure 4(a) and (b), the peak intensity variations for m/e = 16, 42, and 43 amu in the mass spectrum were monitored with increasing the reaction temperature. Details of experimental method were explained in experimental section. As shown in Figure 5, the peak intensities were not seriously changed at lower than 400 °C but started to change at the temperature range of 400-450 °C from the background intensities. This indicates that the DAMI precursor starts to decompose at least above 400 °C, which is consistent with our deposition temperature and the previous FT-IR results.[20] Interestingly, the peak intensity of isopropyl (43 amu) decreased with increasing the reaction temperature, while the peak intensities of methane (16 amu) and propene (42 amu) increased.

In the CVD process with single precursor, various alkyl metal alkoxides [RMO-R] have been usefully applied to deposit metal oxide films without an extra oxygen reactant and the decomposition pathway has been explained by the concept of β-hydrogen elimination in many cases.[4,7] The atomic concentration of Al:O in the deposited film was estimated to be ~1:1.1 in low-pressure CVD process. It may imply that the decomposition mechanism of DMAI is also
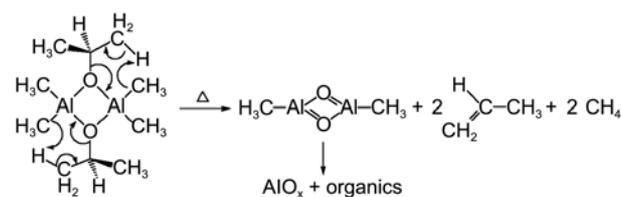
basically governed by β-hydrogen elimination in our CVD process.

In order to understand the intensity variations of mass peaks, the β-hydrogen elimination process can be considered as the thermal decomposition mechanism of DMAI precursor. Concerning with β-hydrogen elimination mechanism, the thermal decomposition of the DMAI can be accomplished by a concerted mechanism with a plausible 6-membered transition state composed of methyl, aluminum, and isopropoxy, in which β-hydrogen (from oxygen) can be abstracted by methyl ligand as explained in Scheme 1. Therefore, methane and 2-propene are expected as by-products and ($OAlCH_3)_2$ as an intermediate state. Simultaneously, the ($OAlCH_3)_2$ should be further decomposed to produce AlO_x (x = 1) as explained in Scheme 1. The increase of peak intensities of m/z = 16 and 42 and the decrease of peak intensities of m/z = 43 were well explained by β-hydrogen elimination process suggested in Scheme 1.

The Al-O bond (511 kJ/mol) is much stronger than Al-C bond (272 kJ/mol) and the dissociation energy of one methyl in the trimethylaluminum [$Al(CH_3)_3$] was calculated to 334 kJ/mol.[26] Therefore, it is expected that two methyl radicals in ($OAlCH_3)_2$ might be preferably decomposed than Al-O. The decomposed methyl radicals may have several possible reaction pathways, such as the reaction with substrate as contaminant, the recombination with other methyl radicals to produce ethane, and the reaction with other by-products. In our QMS experiment, it is difficult to find a direct evidence for the decomposition process of ($OAlCH_3)_2$ because the mass numbers of expected products by the decomposition and/or the recombination of methyl radicals from ($OAlCH_3)_2$ are also simultaneously contributed by the fragments of other decomposed products of DMAI. However, from the negligible carbon incorporation (less than 2%) in the deposited AlO_x films measured by AES and XPS, the reaction of decomposed methyl radical with the substrate can be ruled out.

Finally, in order to find suitable application of non-stoichiometric AlO_x films controlled from DMAI single precursor for non-volatile resistive memory device, the resistance switching characteristics were measured. Figure 6 shows typical current versus voltage (I-V) curve of a Au/AlO_x/Ir MIM capacitor structure with a 50 nm-thick AlO_x film. Firstly, the initial soft breakdown, what is called "Forming state" occurred at the applied voltage of 12.2 V and the film was maintained to the low resistance state (LRS) without applying an external voltage. With increasing
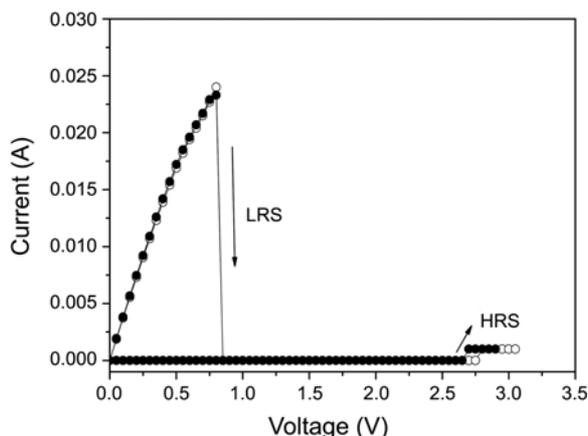
Figure 6. Current-voltage characteristics in the Au/AlOₓ/Ir structure with the AlOₓ films deposited at 450 °C.

applied voltage again at second measurement, the current increased and then suddenly dropped to a low value at 0.8 V (V_{OFF}) as the high resistance state, HLS. With increasing the voltage at third measurement, the HRS was switched to LRS at 2.7 eV (V_{ON}). In this measurement, the leakage currents of Forming state and LRS were limited to prevent a dielectric breakdown of the AlOₓ film by the internal circuit in the source-meter unit. The current ratio between HRS and LRS was larger than $\sim 10^3$, which is possibly applicable to ReRAM device.

Figure 7(a) exhibits the initial states before "electroforming" and the HRS. The unformed and "off" state indicates approximately the similar magnitude of resistance estimated from the diameter of the Cole-Cole plot of Figure 7(a), The high resistance state is believed to originate from the identical electrical response, the resistance of AlOₓ thin films. It should be noted that the AlOₓ thin films are relatively less resistive, if compared to the stoichiometric aluminum oxide, Al_2O_3, *e.g.*, deposited through atomic layer deposition using TMA (trimethyl aluminum) and H_2O.[11] Typically stoichiometric aluminum oxide thin films, *e.g.* TMA-grown Al_2O_3 thin films exhibit extremely high resistivity. Such Al_2O_3 thin films function as purely capacitors, which can be approximated by pseudo-infinite resistance in the equivalent circuit analysis. The insulating features lead to an impedance spectrum where high-frequency impedance data points are situated along the vertical complex line, unlike that of defective AlOₓ thin films, as shown in Figure 7(a). On contrary to the "off" state, the apparent "on" state shows the resistance of 44.8 ohm, taking into account the contribution of the lead wires, *i.e.*, 6.0 ohm. (See Fig. 7(b)). The "on" state resistance reflects that the "on" state is dominated by the filament formation, even though there is significant portion of high resistance portion. The superior conductivity of filaments overwhelms the effect of the high resistance portions. In other words, the impedance spectra reflects that the formation and disconnection of the high-conductive path and that the characteristic capacitance of Figure 7(a) can be attributed to the bulk response, excluding the interfacial contributions to resistive switching phenomena. To explain
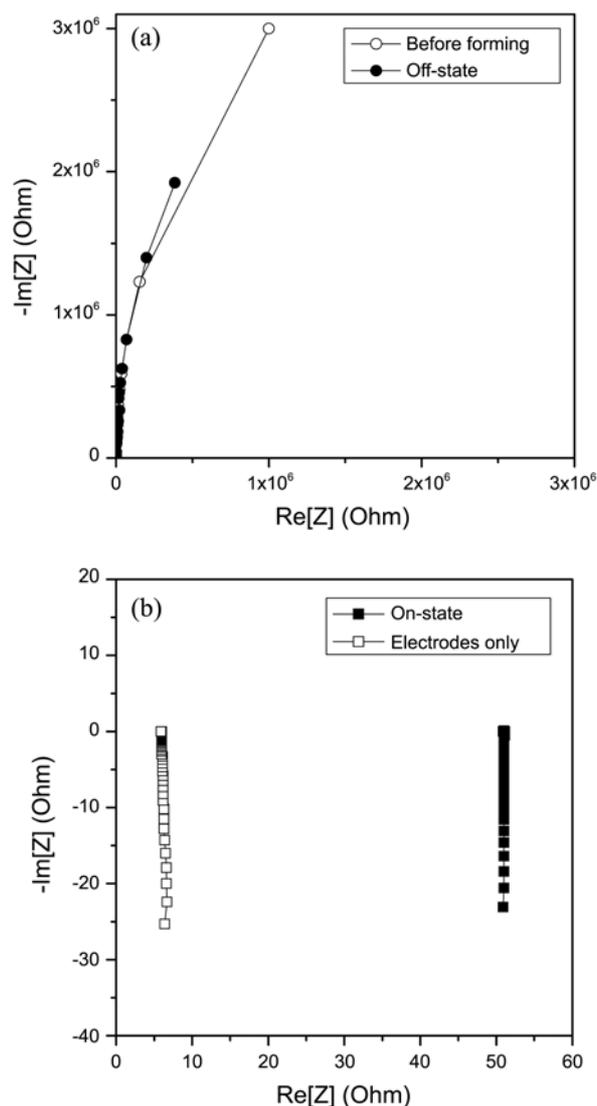
Figure 7. Impedance spectra at the states in the current-voltage characteristics. (a) before forming and off-state after forming and (b) on state after forming along with the lead contributions originating from the characterization system.

the resistive switching behavior, various models have been suggested based on filamentary conductions, charge trapping defect states, trap-controlled space-charge limited current, and the alternation of Schottky barrier. Among these models, the filamentary conducting model is expected to be most appropriate in the current AlOₓ thin films, like the resistive switching features found in the NiO thin films.[27]

Conclusion

We have prepared non-stoichiometric AlOₓ thin films by MOCVD using the single precursor, dimethylaluminum isopropoxide (DMAI, $(CH_3)_2AlO^iPr$), without an extra oxygen source. The atomic concentration of Al and O in the deposited films was measured to be Al:O = ~1:1.1 that is almost the same as that of the single precursor. The dominant reaction mechanism has been presumably suggested to be β-

hydrogen elimination process. The current-voltage characteristics of the AlO_x films show high ON/OFF ratio of 10^6 with SET and RESET voltages of 2.7 and 0.8 V, respectively.

References

1. Hitchman, M. L.; Jenson, K. F. *Chemical Vapor Deposition: Principle and Applications*; Academic Press: New York, 1993.
2. Cowley, A. H.; Jones, R. A. *Angew. Chem. Int. Ed. Engl.* **1989**, *28*, 1208.
3. Auld, J.; Houlton, D. J.; Jones, A. C.; Rushworth, S. A.; Malik, M. A.; O'Brien, P.; Critchlow, G. W. *J. Mater. Chem.* **1994**, *4*, 1249.
4. Sung, M. M.; Kim, C.; Kim, C. G.; Kim, Y. *J. Cryst. Growth* **2000**, *210*, 651.
5. Koh, W.; Ku, S.-J.; Kim, Y. *Thin Solid Films* **1997**, *304*, 222.
6. Sung, M. M.; Kim, C.; Yoo, S. H.; Kim, C. G.; Kim, Y. *Chem. Vap. Deposition* **2002**, *8*, 50.
7. Ashby, E. C.; Willard, G. F.; Goel, A. B. *J. Org. Chem.* **1979**, *44*, 1221.
8. Dong, R.; Lee, D. S.; Xiang, W. F.; Oh, S. J.; Seong, D. J.; Heo, S. H.; Choi, H. J.; Kwon, M. J.; Seo, S. N.; Pyun, M. B.; Hasan, M.; Hwang, H. *Appl. Phys. Lett.* **2007**, *90*, 042107.
9. Lee, D.; Choi, H.; Sim, H.; Choi, D.; Hwang, H.; Lee, M.-J.; Seo, S.-A.; Yoo, I. K. *IEEE Elec. Dev. Lett.* **2005**, *26*, 719.
10. Jeong, K. W.; Do, Y. H.; Yoon, K. S.; Kim, C. O.; Hong, J. P. *J. Korean Phys. Soc*. **2006**, *48*, 1501.
11. Cho, W.; Sung, K.-W.; An, K.-S.; Lee, S. S.; Chung, T.-M.; Kim, Y. *J. Vac. Sci. Technol. A* **2003**, *21*, 1366.
12. Park, J.-W.; Kim, D.-Y.; Lee, J.-K. *J. Vac. Sci. Technol. A* **2005**, *23*, 1309.
13. Park, J.-W.; Jung, M. K.; Yang, M. K.; Lee, J.-K. *J. Vac. Sci. Technol. B* **2006**, *24*, 2205.
14. Choi, B. J.; Choi, S.; Kim, K. M.; Shin, Y. C.; Hwang, C. S.; Hwang, S.-Y.; Cho, S.-S.; Park, S.; Hong, S.-K. *Appl. Phys. Lett.* **2006**, *89*, 0129060.
15. Sim, H.; Choi, D.; Lee, D.; Hasan, M.; Samantaray, C. B.; Hwang, H. *Microelec. Engin.* **2005**, *80*, 260.
16. Bardhan, A. R.; Srivastava, P. C.; Bhattacharya, D. L. *Thin Solid Films* **1974**, *24*, S41.
17. Lin, C.-Y.; Wu, C.-Y.; Wu, C.-Y.; Hu, C.; Tseng, T.-Y. *J. Electrochem. Soc.* **2007**, *154*, G189.
18. Watanabe, Y.; Bednorz, J. G. J.; Bietsch, A.; Gerber, C.; Widmer, D.; Beck, A. *Appl. Phys. Lett.* **2001**, *78*, 3738.
19. Beck, A.; Bednorz, J. G.; Gerber, C.; Rossel, C.; Widmer, D. *Appl. Phys. Lett.* **2000**, *77*, 139.
20. Barreca, D.; Battiston, G. A.; Gerbasi, R.; Tondello, E. *J. Mater. Chem.* **2000**, *10*, 2127.
21. Lee, S. Y.; Luo, B.; Sun, Y.; White, J. M.; Kim, Y. *Appl. Surf. Sci.* **2004**, *222*, 234.
22. Kottler, V.; Gillies, M. F.; Kuiper, A. E. T. *J. Appl. Phys.* **2001**, *89*, 3301.
23. Taylor, J. A. *J. Vac. Sci. Tech.* **1982**, *20*, 751.
24. Rogers, J. H.; Apblett, A. W.; Cleaver, W. M.; Tyler, A. N.; Barron, A. R. *J. Chem. Soc. Dalton Trans.* **1992**, 3179.
25. He, G.; Zhang, L. D.; Fang, Q. *J. Appl. Phys.* **2006**, *100*, 083517-1.
26. Handbook of Chemistry and Physics 76th CRC press.
27. Seo, S.; Lee, M. J.; Seo, D. H.; Jeoung, E. J.; Suh, D.-S.; Joung, Y. S.; Yoo, I. K.; Hwang, I. R.; Kim, S. H.; Byun, I. S.; Kim, J.-S.; Choi, J. S.; Park, B. H. *Appl. Phys. Lett.* **2004**, *85*, 5655.